Molecular Dynamics Simulations on the Oligomer-Formation Process of the GNNQQNY Peptide from Yeast Prion Protein Sup35

Zhuqing Zhang, Hao Chen, Hongjun Bai, and Luhua Lai
Beijing National Laboratory for Molecular Sciences, State Key Laboratory for Structural Chemistry of Stable and Unstable Species, College of Chemistry and Molecular Engineering; and Center for Theoretical Biology, Peking University, Beijing 100871, China

ABSTRACT Oligomeric intermediates are possible cytotoxic species in diseases associated with amyloid deposits. Understanding the early steps of fibril formation at atomic details may provide useful information for the rational therapeutic design. In this study, using the heptapeptide GNNQQNY from the yeast prion-like protein Sup35 as a model system, for which a detailed atomic structure of the fibril formed has been determined by x-ray microcrystallography, we investigated its oligomer-formation process from monomer to tetramer at the atomistic level by means of a molecular dynamics simulation with explicit water. Although the number of simulations was limited, the qualitative statistical data gave some interesting results, which indicated that the oligomer formation might start from antiparallel β-sheet-like dimers. When a new single peptide strand was added to the preformed dimers to form trimers and then tetramers, the transition time from disorder aggregates to regular ones for the parallel alignment was found to be obviously much less than for the antiparallel one. Moreover, the parallel pattern also statistically stayed longer, providing more chances for oligomer extending, although the number of parallel stack events was almost equal to antiparallel ones. Therefore, our simulations showed that new strands might prefer to extend in a parallel arrangement to form oligomers, which agrees with the microcrystal structure of the amyloid fibril formed by this peptide. In addition, analysis of the π-π stacking of aromatic residues showed that this type of interaction did not play an important role in giving directionality for β-strand alignment but played a great influence on stabilizing the structures formed in the oligomer-formation process.

INTRODUCTION

Amyloid fibrils are highly ordered protein aggregates which are associated with pathologies like Alzheimer's disease, Parkinson's disease, type II diabetes, and transmissible spongiform encephalopathies (1–4). Moreover, it has been known that many proteins with unknown pathogenic roles and some designed or synthetic peptides could also form amyloid fibrils under appropriate conditions (5–9). Although these amyloidogenic proteins do not share any sequence homology or common fold structure, they exhibit a remarkably similar cross β structure, with β-sheet backbones perpendicular to and hydrogen bonds parallel to the fibril axis (1,3). These imply that the underlying physical mechanisms of the assembling process may be common to all amyloidogenic proteins. Recent experiments demonstrated that soluble oligomeric intermediates are more toxic than fully formed mature amyloid fibrils (10–12). Thus designing drugs that can prevent the formation of oligomeric intermediates or make them unstable and turn to mature fibril fast is a major concern in drug discovery against related diseases. However, although great progress has been made on the investigation of amyloid fibril-formation mechanisms (13–17), including those efforts of the advent of amyloid inhibitors (18,19), how the amyloidogenic proteins form oligomers and the mechanism of their toxicity are still elusive.

Due to the noncrystalline and insoluble nature of the amyloid fibrils, it is difficult to determine their atomic resolution structure experimentally. Until recently, only a few of them have been attained by the x-ray microcrystallography data (20,21), by quenched hydrogen-deuterium exchange NMR together with pairwise mutagenesis (22), or by combing a range of biophysical techniques including fluorescence and NMR spectroscopy (23). On the other hand, many short peptides displayed the same amyloid properties as full-length polypeptides, such as GNNQQNY from the yeast prion Sup35 (residues 7–13) (24), NFGAIL from human IAPP (residues 22–27) (25), and DFNKF from human calcitonin (residues 15–19) (26). This inspired intensively experimental and theoretical, especially computational, simulation studies to uncover amyloidgenic protein fibril-formation processes (27–29) or predict the amyloidgenic propensity of different sequences through short core segments (30–32). For example, Melquiond et al. (33,34) studied the mechanism of aggregation of the peptide KFFE, which is the shortest one known to form amyloid fibrils in vitro. Lopez de la Paz et al. (35) investigated the de novo designed amyloidgenic peptide STVIIE and its mutations by molecular dynamics (MD). Additionally, there are also some reports on the aggregation of the short peptide $A\beta_{16-22}$ (36,37). All these studies have improved our understanding of the oligomer-formation mechanism of amyloidogenic peptides to a certain extent.

The fibrous microcrystal of heptapeptide GNNQQNY from the yeast prion-like protein Sup35, determined by Eisenberg and co-workers (21), reveals a parallel arrangement

Submitted November 4, 2006, and accepted for publication April 25, 2007.

Address reprint requests to Luhua Lai, College of Chemistry and Molecular Engineering Peking University, Beijing 100871, China. Tel.: 86-10-62757486; Fax: 86-10-62751725; E-mail: lhlai@pku.edu.cn.

Editor: Ruth Nussinov.

0006-3495/07/09/1484/09 $2.00

doi: 10.1529/biophysj.106.100537

of β-strands perpendicular to the fibril axis and provides a good model to study the amyloid formation. For this peptide, there have been several MD simulation studies on the very early steps of the fibril-formation event (38–40), the thermodynamic stability of different sizes of oligomers (41,42), as well as the driving force of the fibrillogenic association (43). Gsponer et al. (39) observed that the parallel β-sheet arrangement was favored over the antiparallel one due to side-chain contacts by using implicit solvent MD simulations with three peptides starting from random conformations and orientations. Taking the crystal structure determined by Eisenberg et al. as initial conformations, Zheng and coworkers (42) studied the stability of the heptapeptide oligomers with different sizes by explicit solvent MD simulations and found that the parallel two-strand β-sheet is much more unstable than corresponding trimers and tetramers. Then how does the aggregation process occur from monomer to dimer then to larger oligomers? In this study, all-atom MD simulations with an explicit solvent model were performed to investigate the oligomer-formation processes of the heptapeptide GNNQQNY from monomer to tetramer by adding one peptide at each step. Similar to Zheng et al.'s simulations, we also found the parallel β-sheet dimers unstable, whereas antiparallel arrangement is more favored in most of the dimerization simulations. However, from dimer to trimer and tetramer, parallel stacking of newly introduced strands were found to be more favored, which accords well with the experimental matured microcrystal structure.

MATERIALS AND METHODS

All MD simulations were carried out by using the GROMACS 3.3 software package (44,45) with constant number, pressure, and temperature and periodic boundary conditions. -The GROMACS96 force field (46) was applied. The models were immersed in rectangular or cubic boxes filled with water molecules with a distance between peptides and box edges of at least 10 Å. A simple point-charge water model (47) was used for the solvent molecules in the simulations. The boxes' sizes for monomer-, dimer-, trimer-, and tetramer-formation simulations is 45 Å $\times$ 25 Å $\times$ 35 Å, 60 Å $\times$ 60 Å $\times$ 60 Å, 65 Å $\times$ 65 Å $\times$ 65 Å, and 75 Å $\times$ 75 Å $\times$ 75 Å, respectively, and the corresponding number of water molecules are ~1045, 7080, 9010, and 13,670. The linear constraint solver (LINCS) method (48) was used to constrain bond lengths, allowing an integration step of 2 fs. Electrostatic interactions were calculated with the particle mesh Ewald algorithm (49,50). The cutoff radius for the Lennard-Jones interactions was set as 10 Å. The simulations were performed at 300 K except that the monomer simulation was set at 450 K. The Berendsen algorithm (51) has been applied for temperature and pressure coupling. Most of the analyses were performed by using facilities within the GROMACS package. Secondary structure analyses were carried out employing the defined secondary structure of proteins (DSSP) method (52). All images were produced by using the software PyMOL (53).

A 6 ns MD simulation of monomer at 450 K was first performed with initial coordinates taken from the x-ray crystal structure (Protein Data Bank code 1YJP) (21) to sample all the possible conformations. The oligomer formations from dimer to tetramer were performed by MD by adding one peptide at each step, except for tetramer formation in which some initial conformations were the combination of two dimers. All the starting conformations are schematically shown in Fig. 1. In each initial structure of all the simulations, the newly added peptide, possessing random conformation and orientation, was extracted from the monomer MD trajectory, and the dimers, trimers for trimer, and tetramer formation were extracted from dimer- or trimer-formation trajectories. The distance of the two separated parts was >10 Å at the beginning, as the cutoff of 10 Å for the Lennard-Jones interaction was adopted. In this study, a total of 30 independent dimer-formation simulations with each running for 50 ns, 20 independent trimer-formation simulations with each running for 70 ns, and 21 independent tetramer simulations (7 for each type of initial conformations) with each running for 80 ns was carried out.

RESULTS

Dimer formation

In each of the 30 dimerization simulations, the two peptides with random orientations and conformations, both extracted from the monomer MD trajectory, were separated from each other by at least 10 Å initially, as this distance was the cutoff value for the Lennard-Jones interaction (see the Materials and Methods section). Fig. 1 *a* shows the schematic initial structure. Under the simulation conditions as described in the Materials and Methods section, the two peptides moved close to each other, then aggregated. The aggregation time was estimated when the mass centers distance of the two peptides decreased to <10 Å, and it varied greatly from 2 ns to 38 ns in the 30 simulations (Figure S1 in Supplementary Material). As the analysis of secondary structure showed

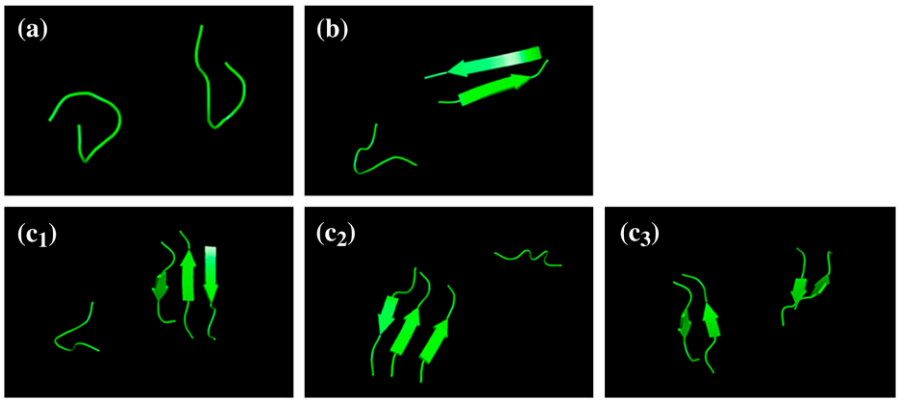

FIGURE 1 The schematic initial structures used in the simulation study. (*a*) For dimer formation: two peptides with random conformations and orientations. (*b*) For trimer formation: one antiparallel two-strand β-sheet extracted from dimer-formation simulation and one monomer. (c_1–c_3) For tetramer formation: (c_1) one antiparallel three-strand β-sheet from trimer-formation trajectory and one monomer; (c_2) one three-strand β-sheet with two nearby parallel strands and an antiparallel strand at one side and one monomer; (c_3) two antiparallel two-strand β-sheets extracted from dimer-formation trajectories.

(Figure S2), after aggregation, most of the two peptides formed obvious β-like structure. We also checked the number of backbone-backbone hydrogen bonds formed between the two peptides (Figure S3) and found that in most cases, when two peptides aggregate, backbone hydrogen interaction between them begins to occur, and four hydrogen bonds or more correspond to a β-sheet conformation.

In the 30 independent dimerization simulations, obvious β-sheet structures were observed in 25 of them. Among these 25 simulations, 22 simulations gave antiparallel β-sheet dimers, most of which stayed until the end of the trajectories, whereas parallel ones were observed in 4 of them. In one of the simulations, a transition from parallel to antiparallel stack was observed. The total occurrence time was ~406 ns and 52 ns for the antiparallel and the parallel alignment, respectively. In both alignments, the distance between the two peptide backbones is ~4.5–5 Å, which is consistent with the distance of 4.87 Å determined by x-ray microcrystallography (21). For the antiparallel dimers in the 22 simulations, there were mainly two kinds of typical structures, as shown in Fig. 2. In the major structure type, the two strands matched perfectly well (Fig. 2 a_1), and in the minor one, there was a little sliding between two strands along the backbone (Fig. 2 a_2).

In one of the simulations, a transition from parallel to antiparallel alignment was observed. As shown in Fig. 3, at ~19.2 ns, the two peptides arranged in parallel at one end (Fig. 3 *a*); after another 7.5 ns, the β-like structure began to deteriorate (Fig. 3 *b*); then at ~36.4 ns, an antiparallel arrangement was formed (Fig. 3 *c*). Although this transition was observed only in one of the simulations, when we extracted two of the parallel β-like structures formed in trajectories as initial ones to carry out another two independent 40 ns MD simulations, this parallel to antiparallel arrangement transition was observed in both of the new simulations. Therefore, we believe that the antiparallel dimer might be easier to form than the parallel one for this heptapeptide.

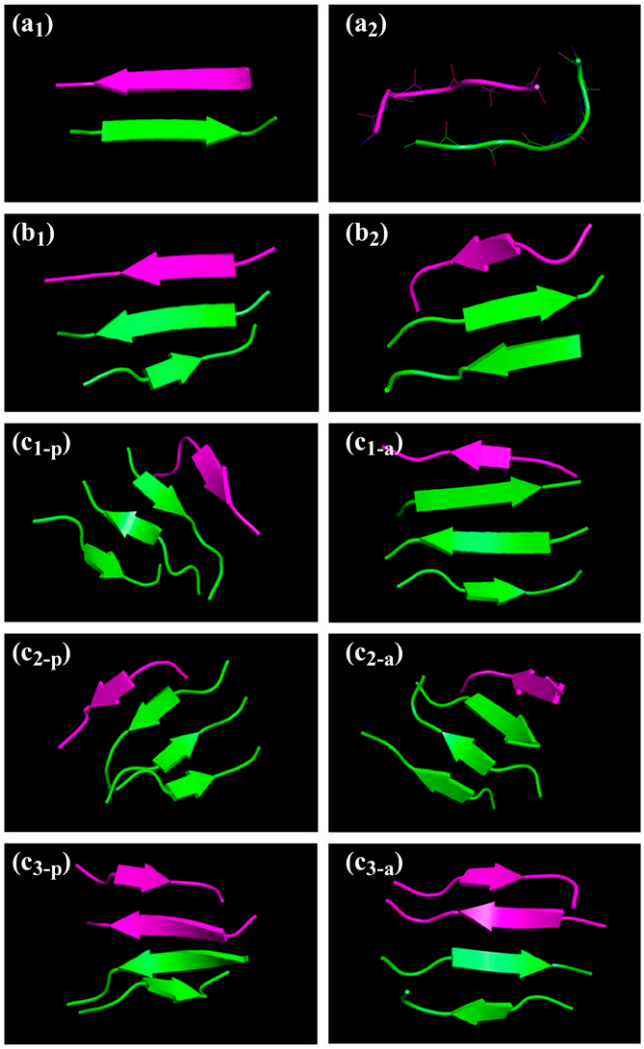

FIGURE 2 The typical β-sheet structures formed in the oligomer simulations. Dimer: (a_1) the two strands matched well; (a_2) a slide along the backbones between the two strands. Trimer: the new strand stacked in parallel (b_1) and in antiparallel (b_2) arrangement. Tetramer: the new strand aligned in parallel ($c_{1\text{-p}}$, $c_{2\text{-p}}$, and $c_{3\text{-p}}$) and in antiparallel ($c_{1\text{-a}}$, $c_{2\text{-a}}$, and $c_{3\text{-a}}$) arrangement. The secondary structure of the new strand is represented in magenta and that of the others is represented in green.

Trimer formation

The schematic starting structures for trimer-formation simulations were shown in Fig. 1 *b*, which were built by putting an assembled antiparallel β-sheet dimer (selected from the above dimer-formation simulations) and a new peptide with random conformation and orientation (from monomer simulation) into the water box with their separation distance of at least 10 Å. Twenty independent 70 ns MD runs were performed. Secondary structure analysis showed that the new peptide arranged along the two-strand β-sheet in parallel alignment in 6 of the 20 simulations and in antiparallel alignment in 8 of them. In one simulation, both parallel and antiparallel alignments were observed, that is, a transition from parallel to antiparallel arrangement occurred. The rest of the simulations exhibited disordered aggregates or the newly introduced strand just congregated with the dimer irregularly. Altogether, parallel and antiparallel structures were observed to stay for ~285 ns and 112 ns in all 20 simulations, respectively, and both of the typical β-like structures were shown in Fig. 2, b_1 and b_2. Obviously, the duration of the parallel alignment is much longer than the antiparallel one.

As the aggregation time was controlled by the diffusion of the two separate groups in water and the congregated time varied significantly in different simulations, how long did it take for the aggregates from disorder to become regular β-like structures? Here, we define a parameter τ termed ''β-like structure-formation time'', which is the difference between β-like structure appearing time and the time of peptides aggregation,

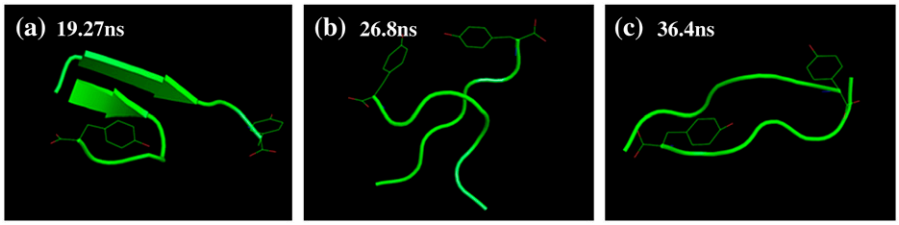

FIGURE 3 Representative snapshots of the transition from parallel to antiparallel arrangement in one dimer-formation trajectory. (*a*) At 19.27 ns, the parallel arrangement was formed at one end; (*b*) the parallel packing was destroyed at ~26.8 ns; (*c*) at ~36.4 ns, the two-strand packed in antiparallel alignment. Only the residue tyrosine is presented in line.

$$\tau = \text{the time the } \beta\text{-like structure appeared} - \text{the time of aggregation.}$$

β-like structure appearing time was measured by secondary structure analysis. Meanwhile, the time of aggregation was determined by when the mass centers distance of two parts was <10 Å. Fig. 4 gives one typical example of mass centers distance measurement of two separated parts and the secondary structure analysis to determine β-like structure-formation time. When comparing the values of this parameter in the simulations where regular three-strand β-sheets formed, as shown in Table 1, we found that for parallel arrangement of the newly introduced strand, the values were remarkably smaller than those for antiparallel arrangement, with an average of 6.7 ns vs. 23.5 ns, although the fluctuation was evident.

Therefore, the trimer-formation simulations showed that parallel increment structure forms faster and stays longer than antiparallel structure.

Tetramer formation

Simulations on the tetramer formation were started from three types of conformations as shown in Fig. 1, c_1–c_3. The first one was constructed by adding a new peptide with conformation from the monomer trajectory and one antiparallel three-strand β-sheet from trimer-formation trajectories (Fig. 1 c_1). The second one was constructed with a three-strand β-sheet with two nearby parallel strands and an antiparallel strand at one side, adding a new monomer with random structure (Fig. 1 c_2). The third one consisted of two two-strand antiparallel β-sheets from dimer-formation trajectories (Fig. 1 c_3). For each type of the initial structures, seven independent 80 ns MD runs were performed.

In 11 of the 21 simulations, regular four-strand β-sheet structures were observed, including parallel alignment of the newly introduced peptides in 7 simulations (four initial structures like that in Fig. 1 c_1, two like that in Fig. 1 c_2, and one like that in Fig. 1 c_3) and antiparallel alignment in 5 simulations (one initial structure like that in Fig. 1 c_1, two like that in Fig. 1 c_2, and two like that in Fig. 1 c_3). In one simulation, the transition from parallel to antiparallel was observed. Altogether, parallel and antiparallel alignment lingered ~175 ns and 128 ns, respectively, and Fig. 2, $c_{1\text{-p}}$–$c_{3\text{-p}}$ and $c_{1\text{-a}}$–$c_{3\text{-a}}$, showed the typical regular structure snapshots observed in these trajectories. We also estimated the β-like structure-formation time τ as mentioned above in the trimer-formation simulations, and the results are also listed in Table 1. It is obvious that the values of τ for parallel arrangement of the newly introduced peptide are also smaller than those for antiparallel ones, with an average of 4 ns compared to 25.8 ns. Although the deviation from the average values is large, this obvious difference indicates that the newly added peptide might prefer parallel increment to the existing β-sheet kinetically.

In the tetramer-formation simulations, a two-layered structure with one extended strand aligning along the side of a three-strand β-sheet, as shown in Fig. 5, was observed distinctly in 4 of the 21 simulations. The side strand stacked in parallel to the middle one of the three-strand β-sheet in

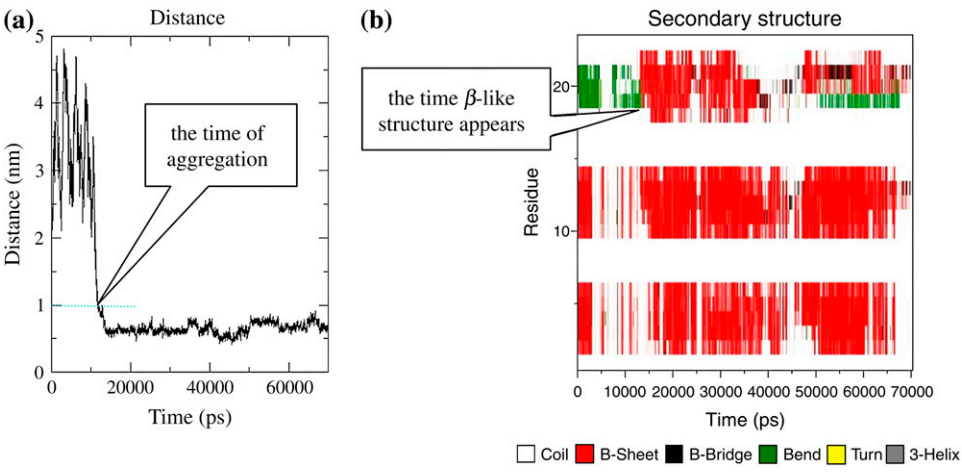

FIGURE 4 Example for β-like structure-formation time definition. (*a*) The change of mass center distance of two separated groups along with time (if this distance is <10 Å, the two groups are considered to form an aggregation); (*b*) the change of secondary structures along with time. The β-like structure-formation time is determined by the difference of the two values obtained in (*b*) and (*a*). Secondary structures were analyzed using DSSP, and β-sheet structures are shown in magenta.

TABLE 1 The β-like structure-formation time in trimer- and tetramer-formation simulations

Oligomers	Arrangement of new peptide	β-like structure formation time (ns)	Average (ns)
Trimers	Parallel	1, 10, 14, 11, 2, 2	6.7 ± 5.1
	Antiparallel	39, 17, 44, 18, 3.5, 15, 28	23.5 ± 13.2
Tetramers	Parallel	2(c_1), 0(c_1), 0(c_1), 18(c_1), 2(c_2), 2(c_2), 4(c_3)	4.0 ± 5.8
	Antiparallel	12(c_2), 17(c_2), 52(c_3), 22(c_3)	25.8 ± 15.5

c_1–c_3 represent simulations corresponding to different initial structures in Fig. 1.

one of the four simulations and in antiparallel in the other three simulations. On average, the two layers were separated by ~8 Å, very close to the 8.5 Å determined in microcrystal structure (21). In this kind of conformation, the complementary shape formed by side-chain amide groups has been observed in some snapshots, just as shown in Fig. 5, *d* and *e*, which is also similar to the observation in the microcrystal structure (21). For each of the four simulations, the root mean-square deviation (RMSD) of backbone atoms, with the most perfect two-layered conformation in each trajectory as reference, was monitored (shown in Figure S4). The total time for RMSD value >0.3 nm was ~78 ns, showing that this kind of conformation lingered for considerable time. Therefore, the second layer might start from tetramers in fibril oligomer formation.

π-π stacking of Tyr side-chain groups

As there is an aromatic residue Tyr in this hexapeptide, we also monitored the π-π stacking conformation in the simulations. Three criteria were used to define a π-π stacking conformation. The distance of the two aromatic rings' geometrical centers should be <6 Å. The angle between the planes of the two aromatic rings should be <45°. The angle between two vectors—one is the average of the two normal vectors to the two aromatic ring planes, the other is the coordinate vector of two aromatic ring geometric centers—should be <60°. We monitored the π-π stacking conformation that satisfied all three criteria in the dimer- and trimer-formation simulations.

For dimer formation, in 11 of all the 25 simulations where β-sheet-like structure was observed, the occurrence time for π-π stacking of Tyr residues was >1 ns, and with a total time of 70 ns for all the 11 trajectories. This structure appeared not only in the irregular aggregates (statistically ~19 ns) but also in the duration of β-sheet formation (statistically ~51 ns). Fig. 6, a_1 and a_2, showed the typical examples of π-π stacking in these two cases.

Meanwhile, for trimer formation, there were 13 simulations in each of which after the two separate parts aggregated, the occurrence time of π-π stacking conformation was >1 ns. There were mainly two cases. One was in the three-strand β-sheet where the introduced strand stacked in parallel alignment (totally 41 ns or so), as the typical example shows in Fig. 6 b_1. The other was in the aggregates where the newly introduced strand had not been aligned along the dimer regularly, but its residue Tyr touched one of the dimers and formed a π-π stacking structure with it (in total 27 ns or so), as shown in Fig. 6 b_2. In the latter, the event occurred in the simulations where eventually the newly introduced strand increased in parallel (duration of the π-π stacking conformation ~10.2 ns), antiparallel (duration ~7.9 ns), as well as irregular arrangement (duration ~8.8 ns). It shows there is no preference for the parallel increment pattern in this case.

Twisting β-sheet conformation

Twisting β-sheet conformation was also observed in many snapshots of dimer-, trimer-, and tetramer-formation processes,

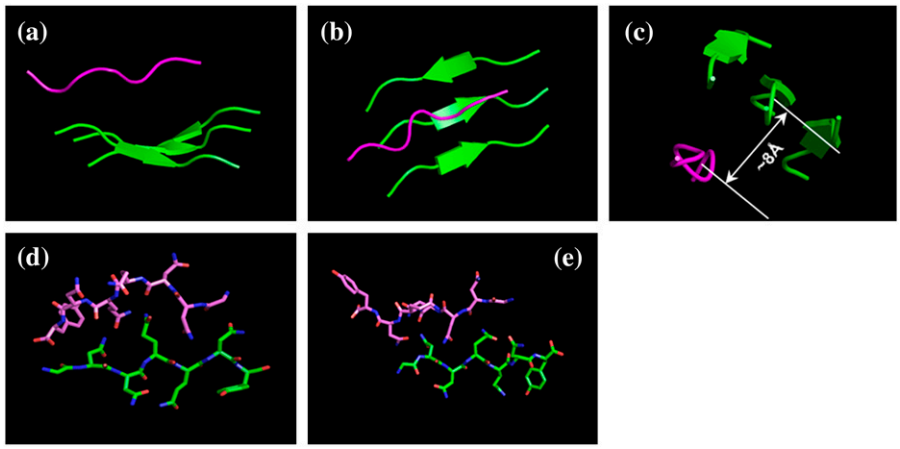

FIGURE 5 The schematic structures of the two-layered conformation observed in tetramer-formation simulations. (*a–c*) The schematics from the view of three orthogonal directions and only main chains are shown, in (*c*) the distance between the two layers is presented ~8 Å; (*d*) and (*e*) are representative conformations of the side strand and the middle one of the three-strand β-sheet (the other two strands within the sheet were hidden) in two independent trajectories, which displayed obviously complementary shape between the two peptides' side-chain groups. The pink represented the side strand, and the green represented the strands in three-strand β-sheet.

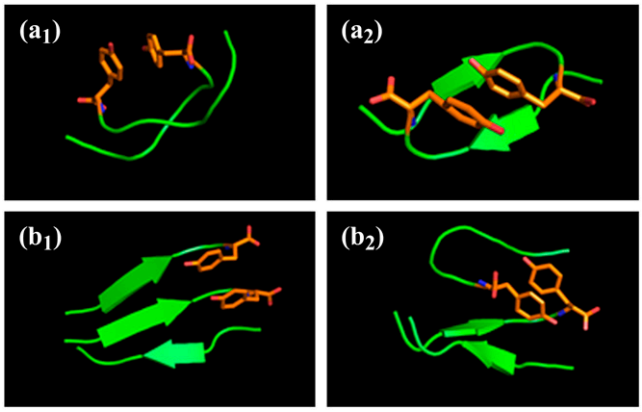

FIGURE 6 The representative π-π stacking conformations in dimer-formation simulations: (a_1) irregular dimer aggregate and (a_2) antiparallel β-sheet dimer, and in trimer-formation simulations: the newly introduced strand (b_1) arranged in parallel and (b_2) coalesced irregularly. The tyrosine residues forming π-π stacking were represented by stick in orange, and other residues were characterized in green.

as the typical schematic examples show in Fig. 7. This indicates that the twisting β-sheet conformation might start from the beginning of the fibril formation, that is, the growing process of very small oligomers.

DISCUSSION

The atomic structure of the cross-β spine of the seven-residue peptide GNNQQNY from Sup35 was determined by Eisenberg and co-workers from its closely related microcrystals (21), which provides important information for amyloid-formation studies. The structure contains a double β-sheet and the parallel segments stack in register within each sheet. Taking conformations from the crystal structures, Zheng et al. performed all-atom explicit solvent MD simulations of various sizes of the peptide oligomers to investigate their stability (42). They found that the parallel two-strand β-sheet conformations were unstable when simulated alone, whereas the parallel β-sheet containing more than two strands were much more stable. Then how do the peptides form the fibrous oligomers from monomers? What kind of dimer conformation should be developed first? We have tried to answer this question in this study. In our dimer-formation MD simulations of this peptide, 22 of the 30 independent trajectories displayed the antiparallel arrangement β-sheet. Furthermore, in one simulation, a transition from parallel to antiparallel alignment was observed. Two additional simulations starting from parallel conformations extracted from the dimer-formation trajectories also showed the same transition. These results are consistent with Zheng et al.'s simulations, which show that the parallel dimers are unstable, implying that the nucleation of amyloid fibrils might start from the antiparallel dimer structure. Although the extended regular β conformation might not be the most energetically stable structure, it can serve as a template to bind new peptides. Thus the kinetically trapped state might be metastable intermediates which play an important role in the formation of early aggregates, just as discussed by Hwang et al. (28).

Many studies have reported on the dimer formation of various short peptides, not only from a kinetic point of view (28,54) but also from a thermodynamic one (55–57). For some peptides, such as $A\beta_{16–22}$, thermodynamic investigation (56) showed its free energy surfaces were complicated, and diverse states with low energy were captured. Although for the GNNQQY peptide, as we focused mainly on its aggregation mechanism, the question of whether the antiparallel dimer preponderantly trapped in the simulations should accompany a complete downhill profile in the free energy surface would need a further thermodynamic study. The different sequence characteristics of the peptide GNNQQNY, which is hydrophilic and comprises no charged residues, may bring some differences compared to those peptides with hydrophobic or electrostatic interactions playing dominating roles in the oligomer assembling process.

Although the soluble oligomer intermediates were thought to be cytotoxic, their formation mechanism is still obscure. Our dimer simulations showed that the two peptides preferred to form antiparallel arrangement, then how do the dimers increase into trimer then tetramer and then form a cross-β-sheet fibril with parallel strands within each sheet? We simulated the trimer- and tetramer-formation process by adding one new peptide to the assembled regular dimer at each step. In these simulations, both parallel and antiparallel alignments of the new peptide were observed. The lingering time of the two patterns was monitored. As indicated by Hwang et al.'s study (28), the dimer structure might be controlled by kinetics; the same might be true for the oligomers like trimer or tetramer. If one type of regular conformation could hold longer than others, then it might have more chances to continue the aggregation. This did occur to the parallel increment in our trimer and tetramer simulations. The other monitor was the comparison of the β-like

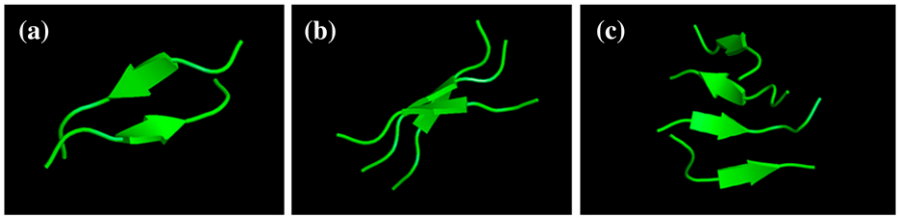

FIGURE 7 The typically schematic twist structures in (a) dimer, (b) trimer, and (c) tetramer aggregates.

structure-formation time, that is, the transition time of aggregates from disorder to regular structure, which also suggested that the parallel alignment was more favorable than the antiparallel one, as for the former, the formation time was apparently shorter.

Therefore, although the number of trajectories for the parallel increment is almost the same as that for the antiparallel one, the two monitors showed that new peptide might add in parallel arrangement more easily, which agrees with the microcrystal structure determined by Eisenberg and co-workers in which the strands are parallel within the β-sheet of the fibril. Gsponer and co-workers (39) performed implicit solvent MD simulations of this peptide starting from three peptide replicas with random conformations, positions, and orientations. They observed a more stable parallel two-strand sheet and all parallel three-strand β-sheet, so they concluded that the parallel β-sheet arrangement is favored over the antiparallel one. The differences between their simulations results and ours might primarily come from the different solvent models used. Instead of the implicit solvent model they used, we adopted an explicit water model, as the important role of water molecules has been reported (58,59). Another reason might arise from the secondary structure bias of different force fields, as some studies have shown that the CHARMM22 is α-helix biased and GROMOS force field is β conformation biased (60,61). This force field β-sheet bias may inevitably drive aggregates toward the ordered β-sheet forms, whereas because our effort is to investigate the prevalence of parallel versus antiparallel species and their roles in amyloid fibril formation and because the peptide conformations are almost identical in parallel and antiparallel β-sheets, the force field bias is not expected to play major roles here.

As the model peptide GNNQQNY is quite hydrophilic, the driving force for oligomer formation should not be hydrophobic interactions as for those highly hydrophobic peptides. Zheng et al. suggested that the driving force might be interstrand backbone-backbone and side-chain side-chain hydrogen bonds within sheet and shape complementary of side chains between sheets (42). Fernandez and co-workers demonstrated that the dipole-dipole interactions play an important role (43). The formation of antiparallel dimer and then parallel increase in our simulations may also come from the interstrand backbone-backbone hydrogen bonds and side-chains interactions. Other studies have shown that π-π stacking of aromatic residues plays an important role in the formation of amyloid fibril structures (17,20,39,40,62–65). Some investigators (62,63,65) proposed that interactions between aromatic residues not only contribute significantly to the thermodynamic stability of the amyloid structures but also provide order and directionality in the self-assembly.

For the peptide GNNQQNY, if it is true, the π-π stacking conformation should be favorable in parallel alignment. Although, in this study, as described in the ''π-π stacking of Tyr side-chain groups'' section, in dimer-formation simulations, this kind of conformation was exhibited not only in antiparallel β-sheet structure, but also in the aggregates before the β-sheet formation, that is, the π-π stacking does not help the strands' arrangement in parallel. Moreover, in trimer-formation processes, before the regular structure formed, the π-π stacking structure was observed both in those parallel increase and those antiparallel increase trajectories, as well as the irregularly aggregates ones, which indicates that aromatic residues may not play an important role in giving directionality to the oligomer-formation process. However, this conformation exhibited a considerably long duration in those parallel increase simulations (almost 41 ns as described previously), which suggests that the aromatic residues might have a considerable influence on the stability of the oligomeric β-sheet structure formed. Gsponer et al. (39) also indicated that aromatic residue does not give directionality to the self-assembly process but stabilizes the parallel aggregates.

It is worth mentioning that, in our simulations, the twisting β-sheet structure was observed in dimer, trimer, and tetramer structures. The twisting structure in amyloid fibrils has been reported in a number of experimental and modeling studies (41,66–68). So our results imply that the twisting β-sheet conformation might begin with the oligomers, even a dimer. Additionally, the two-layered structure was observed lingering considerable time in tetramer-formation simulations, and the complementary conformation of side-chain groups agreed well with the microcrystal structure, suggesting the new layer for the oligomers might start from tetramer aggregates.

In the simulations here, the transition from one aligned pattern to another was observed only in three of the simulations (in dimer, trimer, and tetramer formation, respectively). Furthermore, as the number of simulations was limited due to the limitation of computational power for the all-atomic molecular dynamics with the explicit solvent model, the statistical results were only qualitative. More simulation trajectories with more statistical events may generate better results.

In summary, we have investigated how the small oligomers were formed in the amyloid fibril-formation process of the peptide GNNQQNY from the yeast prion-like protein Sup35 by molecular dynamics simulations. Our simulations suggested that the antiparallel dimer may form first, then new peptides may add to the assemblies in parallel arrangement. Possible reasons for why parallel dimer is not stable and parallel trimers and tetramers are stable were discussed.

SUPPLEMENTARY MATERIAL

To view all of the supplemental files associated with this article, visit www.biophysj.org.

The authors thank Peking University Center for Computational Science and Engineering for providing their computational facility.

This work was supported in part by the National Key Basic Research Project of China (No. 2003CB715900) and National Natural Science Foundation of China (90403001, 30490245).

REFERENCES

1. Dobson, C. M. 1999. Protein misfolding, evolution and disease. *Trends Biochem. Sci.* 24:329–332.
2. Miranker, A. D. 2004. Unzipping the mysteries of amyloid fiber formation. *Proc. Natl. Acad. Sci. USA.* 101:4335–4336.
3. Rochet, J. C., and P. T. Lansbury Jr. 2000. Amyloid fibrillogenesis: themes and variations. *Curr. Opin. Struct. Biol.* 10:60–68.
4. Ross, C. A., and M. A. Poirier. 2004. Protein aggregation and neurodegenerative disease. *Nat. Med.* 10(Suppl):S10–S17.
5. Dobson, C. M. 2002. Getting out of shape. *Nature.* 418:729–730.
6. Fandrich, M., M. A. Fletcher, and C. M. Dobson. 2001. Amyloid fibrils from muscle myoglobin. *Nature.* 410:165–166.
7. Guijarro, J. I., M. Sunde, J. A. Jones, I. D. Campbell, and C. M. Dobson. 1998. Amyloid fibril formation by an SH3 domain. *Proc. Natl. Acad. Sci. USA.* 95:4224–4228.
8. Lopez de la Paz, M., K. Goldie, J. Zurdo, E. Lacroix, C. M. Dobson, A. Hoenger, and L. Serrano. 2002. De novo designed peptide-based amyloid fibrils. *Proc. Natl. Acad. Sci. USA.* 99:16052–16057.
9. Zhang, S., C. Lockshin, R. Cook, and A. Rich. 1994. Unusually stable β-sheet formation in an ionic self-complementary oligopeptide. *Biopolymers.* 34:663–672.
10. Bucciantini, M., E. Giannoni, F. Chiti, F. Baroni, L. Formigli, J. Zurdo, N. Taddei, G. Ramponi, C. M. Dobson, and M. Stefani. 2002. Inherent toxicity of aggregates implies a common mechanism for protein misfolding diseases. *Nature.* 416:507–511.
11. Hardy, J., and D. J. Selkoe. 2002. The amyloid hypothesis of Alzheimer's disease: progress and problems on the road to therapeutics. *Science.* 297:353–356.
12. Silveira, J. R., G. J. Raymond, A. G. Hughson, R. E. Race, V. L. Sim, S. F. Hayes, and B. Caughey. 2005. The most infectious prion protein particles. *Nature.* 437:257–261.
13. Ahmad, A., V. N. Uversky, D. Hong, and A. L. Fink. 2005. Early events in the fibrillation of monomeric insulin. *J. Biol. Chem.* 280:42669–42675.
14. Collins, S. R., A. Douglass, R. D. Vale, and J. S. Weissman. 2004. Mechanism of prion propagation: amyloid growth occurs by monomer addition. *PLoS Biol.* 2:1582–1590.
15. Gsponer, J., and M. Vendruscolo. 2006. Theoretical approaches to protein aggregation. *Protein Pept. Lett.* 13:287–293.
16. Nguyen, H. D., and C. K. Hall. 2004. Molecular dynamics simulations of spontaneous fibril formation by random-coil peptides. *Proc. Natl. Acad. Sci. USA.* 101:16180–16185.
17. Tjernberg, L. O., D. J. Callaway, A. Tjernberg, S. Hahne, C. Lilliehook, L. Terenius, J. Thyberg, and C. Nordstedt. 1999. A molecular model of Alzheimer amyloid beta-peptide fibril formation. *J. Biol. Chem.* 274:12619–12625.
18. Blanchard, B. J., A. Chen, L. M. Rozeboom, K. A. Stafford, P. Weigele, and V. M. Ingram. 2004. Efficient reversal of Alzheimer's disease fibril formation and elimination of neurotoxicity by a small molecule. *Proc. Natl. Acad. Sci. USA.* 101:14326–14332.
19. Gestwicki, J. E., G. R. Crabtree, and I. A. Graef. 2004. Harnessing chaperones to generate small-molecule inhibitors of amyloid β aggregation. *Science.* 306:865–869.
20. Makin, O. S., E. Atkins, P. Sikorski, J. Johansson, and L. C. Serpell. 2005. Molecular basis for amyloid fibril formation and stability. *Proc. Natl. Acad. Sci. USA.* 102:315–320.
21. Nelson, R., M. R. Sawaya, M. Balbirnie, A. O. Madsen, C. Riekel, R. Grothe, and D. Eisenberg. 2005. Structure of the cross-β spine of amyloid-like fibrils. *Nature.* 435:773–778.
22. Luhrs, T., C. Ritter, M. Adrian, D. Riek-Loher, B. Bohrmann, H. Dobeli, D. Schubert, and R. Riek. 2005. 3D structure of Alzheimer's amyloid-beta(1–42) fibrils. *Proc. Natl. Acad. Sci. USA.* 102:17342–17347.
23. Ritter, C., M. L. Maddelein, A. B. Siemer, T. Luhrs, M. Ernst, B. H. Meier, S. J. Saupe, and R. Riek. 2005. Correlation of structural elements and infectivity of the HET-s prion. *Nature.* 435:844–848.
24. Balbirnie, M., R. Grothe, and D. S. Eisenberg. 2001. An amyloid-forming peptide from the yeast prion Sup35 reveals a dehydrated beta-sheet structure for amyloid. *Proc. Natl. Acad. Sci. USA.* 98:2375–2380.
25. Tenidis, K., M. Waldner, J. Bernhagen, W. Fischle, M. Bergmann, M. Weber, M. L. Merkle, W. Voelter, H. Brunner, and A. Kapurniotu. 2000. Identification of a penta- and hexapeptide of islet amyloid polypeptide (IAPP) with amyloidogenic and cytotoxic properties. *J. Mol. Biol.* 295:1055–1071.
26. Reches, M., Y. Porat, and E. Gazit. 2002. Amyloid fibril formation by pentapeptide and tetrapeptide fragments of human calcitonin. *J. Biol. Chem.* 277:35475–35480.
27. Wu, C., H. Lei, and Y. Duan. 2005. Elongation of ordered peptide aggregate of an amyloidogenic hexapeptide NFGAIL observed in molecular dynamics simulations with explicit solvent. *J. Am. Chem. Soc.* 127:13530–13537.
28. Hwang, W., S. Zhang, R. D. Kamm, and M. Karplus. 2004. Kinetic control of dimer structure formation in amyloid fibrillogenesis. *Proc. Natl. Acad. Sci. USA.* 101:12916–12921.
29. Paci, E., J. Gsponer, X. Salvatella, and M. Vendruscolo. 2004. Molecular dynamics studies of the process of amyloid aggregation of peptide fragments of transthyretin. *J. Mol. Biol.* 340:555–569.
30. Thompson, M. J., S. A. Sievers, J. Karanicolas, M. I. Ivanova, D. Baker, and D. Eisenberg. 2006. The 3D profile method for identifying fibril-forming segments of proteins. *Proc. Natl. Acad. Sci. USA.* 103:4074–4078.
31. Rojas Quijano, F. A., D. Morrow, B. M. Wise, F. L. Brancia, and W. J. Goux. 2006. Prediction of nucleating sequences from amyloidogenic propensities of tau-related peptides. *Biochemistry.* 45:4638–4652.
32. Lopez de la Paz, M., and L. Serrano. 2004. Sequence determinants of amyloid fibril formation. *Proc. Natl. Acad. Sci. USA.* 101:87–92.
33. Melquiond, A., G. Boucher, N. Mousseau, and P. Derreumaux. 2005. Following the aggregation of amyloid-forming peptides by computer simulations. *J. Chem. Phys.* 122:174904.
34. Melquiond, A., N. Mousseau, and P. Derreumaux. 2006. Structures of soluble amyloid oligomers from computer simulations. *Proteins.* 65:180–191.
35. Lopez de la Paz, M., G. M. de Mori, L. Serrano, and G. Colombo. 2005. Sequence dependence of amyloid fibril formation: insights from molecular dynamics simulations. *J. Mol. Biol.* 349:583–596.
36. Rohrig, U. F., A. Laio, N. Tantalo, M. Parrinello, and R. Petronzio. 2006. Stability and structure of oligomers of the Alzheimer peptide Aβ16–22: from the dimer to the 32-mer. *Biophys. J.* 91:3217–3229.
37. Klimov, D. K., and D. Thirumalai. 2003. Dissecting the assembly of Aβ16–22 amyloid peptides into antiparallel β sheets. *Structure.* 11:295–307.
38. Cecchini, M., F. Rao, M. Seeber, and A. Caflisch. 2004. Replica exchange molecular dynamics simulations of amyloid peptide aggregation. *J. Chem. Phys.* 121:10748–10756.
39. Gsponer, J., U. Haberthur, and A. Caflisch. 2003. The role of side-chain interactions in the early steps of aggregation: molecular dynamics simulations of an amyloid-forming peptide from the yeast prion Sup35. *Proc. Natl. Acad. Sci. USA.* 100:5154–5159.
40. Lipfert, J., J. Franklin, F. Wu, and S. Doniach. 2005. Protein misfolding and amyloid formation for the peptide GNNQQNY from yeast prion protein Sup35: simulation by reaction path annealing. *J. Mol. Biol.* 349:648–658.
41. Esposito, L., C. Pedone, and L. Vitagliano. 2006. Molecular dynamics analyses of cross-β-spine steric zipper models: β-sheet twisting and aggregation. *Proc. Natl. Acad. Sci. USA.* 103:11533–11538.
42. Zheng, J., B. Ma, C. J. Tsai, and R. Nussinov. 2006. Structural stability and dynamics of an amyloid-forming peptide GNNQQNY from the yeast prion Sup-35. *Biophys. J.* 91:824–833.
43. Fernandez, A. 2005. What factor drives the fibrillogenic association of β-sheets? *FEBS Lett.* 579:6635–6640.
44. Berendsen, H. J. C., D. Vanderspoel, and R. Vandrunen. 1995. GROMACS—a message-passing parallel molecular-dynamics implementation. *Comput. Phys. Commun.* 91:43–56.

45. Van Der Spoel, D., E. Lindahl, B. Hess, G. Groenhof, A. E. Mark, and H. J. Berendsen. 2005. GROMACS: fast, flexible, and free. *J. Comput. Chem.* 26:1701–1718.

46. van Gunsteren, W. F., S. R. Billeter, A. A. Eising, P. H. Hünenberger, P. Krüger, A. E. Mark, W. R. P. Scott, and I. G. Tironi. 1996. Biomolecular Simulation: The GROMOS96 Manual and User Guide. VdF Hochschulverlag an der ETH Zurich, Zurich, Germany.

47. Berendsen, H. J. C., J. P. M. Postma, W. F. van Gunsteren, and J. Hermans. 1981. Interaction models for water in relation to protein hydration. *In* Intermolecular Forces. B. Pullman, editor. Reidel, Dordrecht, The Netherlands. 331–342.

48. Hess, B., H. Bekker, H. J. C. Berendsen, and J. Fraaije. 1997. LINCS: a linear constraint solver for molecular simulations. *J. Comput. Chem.* 18:1463–1472.

49. Darden, T., D. York, and L. Pedersen. 1993. Particle mesh Ewald: an N-log(N) method for Ewald sums in large systems. *J. Chem. Phys.* 98: 10089–10092.

50. Essmann, U., L. Perera, M. L. Berkowitz, T. Darden, H. Lee, and L. G. Pedersen. 1995. A smooth particle mesh Ewald potential. *J. Chem. Phys.* 103:8577–8592.

51. Berendsen, H. J. C., J. P. M. Postma, A. DiNola, and J. R. Haak. 1984. Molecular dynamics with coupling to an external bath. *J. Chem. Phys.* 81:3684–3690.

52. Kabsch, W., and C. Sander. 1983. Dictionary of protein secondary structure: pattern recognition of hydrogen-bonded and geometrical features. *Biopolymers.* 22:2577–2637.

53. DeLano, W. L. 2005. The case for open-source software in drug discovery. *Drug Discov. Today.* 10:213–217.

54. Lei, H., C. Wu, Z. Wang, and Y. Duan. 2006. Molecular dynamics simulations and free energy analyses on the dimer formation of an amyloidogenic heptapeptide from human b2-microglobulin: implication for the protofibril structure. *J. Mol. Biol.* 356:1049–1063.

55. Baumketner, A., and J. E. Shea. 2005. Free energy landscapes for amyloidogenic tetrapeptides dimerization. *Biophys. J.* 89:1493–1503.

56. Gnanakaran, S., R. Nussinov, and A. E. Garcia. 2006. Atomic-level description of amyloid β-dimer formation. *J. Am. Chem. Soc.* 128: 2158–2159.

57. Santini, S., G. Wei, N. Mousseau, and P. Derreumaux. 2004. Pathway complexity of Alzheimer's β-amyloid Aβ16–22 peptide assembly. *Structure.* 12:1245–1255.

58. De Simone, A., G. G. Dodson, F. Fraternali, and A. Zagari. 2006. Water molecules as structural determinants among prions of low sequence identity. *FEBS Lett.* 580:2488–2494.

59. De Simone, A., G. G. Dodson, C. S. Verma, A. Zagari, and F. Fraternali. 2005. Prion and water: tight and dynamical hydration sites have a key role in structural stability. *Proc. Natl. Acad. Sci. USA.* 102:7535–7540.

60. Mu, Y., D. S. Kosov, and G. Stock. 2003. Conformational dynamics of trialanine in water. 2. Comparison of AMBER, CHARMM, GROMOS, and OPLS force fields to NMR and infrared experiments. *J. Phys. Chem. B.* 107:5064–5073.

61. Yoda, T., Y. Sugita, and Y. Okamoto. 2004. Secondary-structure preferences of force fields for proteins evaluated by generalized-ensemble simulations. *Chem. Phys.* 307:269–283.

62. Tjernberg, L. O., J. Naslund, F. Lindqvist, J. Johansson, A. R. Karlstrom, J. Thyberg, L. Terenius, and C. Nordstedt. 1996. Arrest of β-amyloid fibril formation by a pentapeptide ligand. *J. Biol. Chem.* 271:8545–8548.

63. Gazit, E. 2002. A possible role for pi-stacking in the self-assembly of amyloid fibrils. *FASEB J.* 16:77–83.

64. Bemporad, F., N. Taddei, M. Stefani, and F. Chiti. 2006. Assessing the role of aromatic residues in the amyloid aggregation of human muscle acylphosphatase. *Protein Sci.* 15:862–870.

65. Azriel, R., and E. Gazit. 2001. Analysis of the structural and functional elements of the minimal active fragment of islet amyloid polypeptide (IAPP)—an experimental support for the key role of the phenylalanine residue in amyloid formation. *J. Biol. Chem.* 276:34156–34161.

66. Chothia, C. 1973. Conformations of twisted b-sheets in proteins. *J. Mol. Biol.* 75:295–302.

67. Soto, P., J. Cladera, A. E. Mark, and X. Daura. 2005. Stability of SIV gp32 fusion-peptide single-layer protofibrils as monitored by molecular-dynamics simulations. *Angew. Chem. Int. Ed. Engl.* 44:1065–1067.

68. Wang, J. M., S. Gulich, C. Bradford, M. Ramirez-Alvarodo, and L. Regan. 2005. A twisted four-sheeted model for an amyloid fibril. *Structure.* 13:1279–1288.